A geostatistical data fusion technique for merging remote sensing and ground-based observations of aerosol optical thickness

Abhishek Chatterjee,[1] Anna M. Michalak,[1,2] Ralph A. Kahn,[3] Susan R. Paradise,[4] Amy J. Braverman,[4] and Charles E. Miller[4]

Received 23 December 2009; revised 1 July 2010; accepted 12 July 2010; published 23 October 2010.

[1] The Multiangle Imaging Spectroradiometer (MISR) and the Moderate Resolution Imaging Spectroradiometer (MODIS) aboard the NASA Earth Observation System's Terra satellite have been measuring aerosol optical thickness (AOT) since early 2000. These remote-sensing platforms complement the ground-based Aerosol Robotic Network (AERONET) in better understanding the role of aerosols in climate and atmospheric chemistry. To date, however, there have been only limited attempts to exploit the complementary multiangle (MISR) and multispectral (MODIS) capabilities of these sensors along with the ground-based observations in an integrated analysis. This paper describes a geostatistical data fusion technique that can take advantage of the spatial autocorrelation of the AOT distribution, while making optimal use of all available data sets. Using Level 2.0 AERONET, MISR, and MODIS AOT data for the contiguous United States, we demonstrate that this approach can successfully incorporate information from multiple sensors and provide accurate estimates of AOT with rigorous uncertainty bounds. Cross-validation results show that the resulting AOT product is closer to the ground-based AOT observations than either of the individual satellite measurements.

Citation: Chatterjee, A., A. M. Michalak, R. A. Kahn, S. R. Paradise, A. J. Braverman, and C. E. Miller (2010), A geostatistical data fusion technique for merging remote sensing and ground-based observations of aerosol optical thickness, *J. Geophys. Res.*, *115*, D20207, doi:10.1029/2009JD013765.

1. Introduction

[2] Atmospheric aerosols play an important and dynamic role in climate and atmospheric chemistry. The climatic effects of aerosols had already been recognized in the 1970s [*Andreae*, 1995] but the focus of scientific attention shifted only during the late 1980s due to the impact of the growing concentrations of CO_2 and other greenhouse gases. Although the radiative forcing of aerosols is still highly uncertain [*Intergovernmental Panel on Climate Change* (*IPCC*), 2007], it is well understood that aerosols contribute significantly to reflected solar radiation (the aerosol direct effect) and modify cloud properties (the aerosol indirect effect), producing a net cooling of the Earth surface, and can also absorb sunlight, thereby warming the ambient atmosphere. Because aerosols have short atmospheric lifetimes of about a week [*Andreae et al.*, 1986], they have a heterogeneous spatial and temporal distribution. Accurately capturing this heterogeneity, and assessing the impact of tropospheric aerosols on regional and global energy budgets, therefore requires diurnally resolved observations from some combination of satellite and suborbital measurements.

[3] Two space-based instruments that aim to fulfill this need are the Multiangle Imaging SpectroRadiometer (MISR) and Moderate Resolution Imaging Spectroradiometer (MODIS) aboard the NASA Earth Observation System's Terra satellite, which are used to derive observations of the tropospheric aerosol optical thickness (AOT), among other parameters [*Diner et al.*, 1998; *Kaufman et al.*, 1997]. Column AOT is defined as the integral of aerosol extinction from the surface to the top of the atmosphere. Although these two sensors are on the same platform, discrepancies exist between them in retrieved AOT over both land and ocean regions [*Penner et al.*, 2002; *Myhre et al.*, 2005; *Kinne et al.*, 2006]. These discrepancies are due to the differences in assumptions in the retrieval algorithms [*Kahn et al.*, 2007], observed wavelengths and viewing geometries [*IPCC*, 2007], and the spatial resolution of observations [*Xiao et al.*, 2009], among other reasons. Methods for evaluating data from these and other instruments are needed, as are approaches for assessing the information content of these data for providing the best possible representation of the spatial and temporal variability in AOT.

[4] The common way of validating the satellite AOT retrievals has been through the use of the ground-based Aerosol Robotic Network (AERONET) [*Holben et al.*, 1998], which provides sparse but relatively reliable AOT observations. Comparisons between AOT retrieved from

[1]Department of Civil and Environmental Engineering, University of Michigan, Ann Arbor, Michigan, USA.
[2]Department of Atmospheric, Oceanic and Space Sciences, University of Michigan, Ann Arbor, Michigan, USA.
[3]NASA Goddard Space Flight Center, Greenbelt, Maryland, USA.
[4]Jet Propulsion Laboratory, Pasadena, California, USA.

0148-0227/10/2009JD013765

space-based instruments and AERONET data have been used in a variety of contexts to explore the similarities and differences between the MISR and MODIS products. These comparisons have focused on MISR and AERONET [*Liu et al.*, 2004a; *Kahn et al.*, 2005a, 2005b; *Jiang et al.*, 2007; *Chen et al.*, 2008], or MODIS and AERONET [*Chu et al.*, 2002; *Levy et al.*, 2003, 2005; *Remer et al.*, 2005], and have been specifically targeted at refining the retrieval algorithms of the individual sensors for different aerosol regimes.

[5] Several studies have also looked at the discrepancies between MISR and MODIS [e.g., *Abdou et al.*, 2005; *Liu et al.*, 2007; *Prasad and Singh*, 2007; *Vermote et al.*, 2007; *Xiao et al.*, 2009; *Kahn et al.*, 2009], mostly by comparing them with the AERONET measurements. These studies have concluded that the major differences can be attributed to location (for example, retrievals near aerosol source regions and/or presence of clouds, retrievals over land versus water) and the aerosol retrieval algorithms over those locations. Recently, *Kahn et al.* [2009] compared MISR and MODIS data sets, and found strong correlations of 0.9 and 0.7 between MISR and MODIS over ocean and land, respectively. Discrepancies between the instruments were traced back to sampling differences, known algorithmic issues, or other mechanisms contributing to aerosol retrieval error. Some of these mechanisms that have been highlighted previously are aerosol model differences [*Abdou et al.*, 2005; *Kahn et al.*, 2007], the presence of clouds [*Martonchik et al.*, 2004; *Kahn et al.*, 2007; *Xiao et al.* 2009; *Kahn et al.*, 2009], dust [*Kalashnikova and Kahn*, 2006; *Martonchik et al.*, 2004], or biomass burning [*Kahn et al.*, 2005a; *Chen et al.*, 2008], as well as other biospheric and anthropogenic factors [*Prasad and Singh*, 2007; *Xiao et al.*, 2009]. Statistical comparisons have also been carried out between MISR, MODIS and AERONET by *Liu and Mishchenko* [2008] and *Mishchenko et al.* [2009], although some of the statistical techniques used have subsequently been questioned [e.g., *Kahn et al.*, 2009]. Overall, the existing literature has resulted in a complex set of conclusions regarding the ways in which MISR, MODIS, and AERONET record AOT [*Xiao et al.*, 2009]. For example, *Liu et al.* [2007] conclude that MODIS generally retrieves higher AOT relative to MISR over land, whereas both MODIS and MISR tend to underestimate AERONET AOT measurements for AOT higher than about 0.5. Similar underestimation is reported by *Jiang et al.* [2007] and *Kahn et al.* [2005a], whereas others conclude that MISR overestimates AERONET AOT observations over water [e.g., *Liu et al.*, 2004a; *Abdou et al.*, 2005; *Kahn et al.*, 2005b].

[6] Given the limitations inherent to each of the available data streams, combining multiple data types may provide an opportunity to optimally estimate the spatial and temporal distribution of AOT. Some studies have found the correlation between the AOT data from multiple sensors to be sufficiently strong to justify the use of ground-based and space-based observations together [*Liu et al.*, 2004a; *Prasad and Singh*, 2007; *Jiang et al.*, 2007]. However, most of the data fusion attempts have been limited to merging data from multiple space-based instruments, including Level 1B (i.e., radiance) data [*Loeb et al.*, 2006], Level 2 data of geophysical parameters [*Gupta et al.*, 2008] and aerosol optical depth [*Nguyen* 2009], and gridded level 3 data sets [*Acker and Leptoukh*, 2007]. Recently, *Kinne* [2009] presented an approach for integrating a weighted composite of remote sensing AOT observations with AERONET AOT through an empirical averaging procedure.

[7] Given the complementary capabilities of the AERONET, MISR and MODIS sensors (see section 2), it seems natural to investigate whether it is possible to merge data from these different sensors in a statistically rigorous framework to obtain an improved AOT product. Such a product could be used to address scientific issues related to air quality and the radiative effects of aerosols, and in particular, be used to evaluate model predictions of aerosol distributions.

[8] The objective of this work is to investigate the applicability of universal kriging, a simple geostatistical data fusion approach, for merging multiple AOT data sets. The approach yields a statistical best estimate of the AOT spatial distribution, together with a quantification of the associated uncertainty. The estimated AOT distribution is based only on the available AOT data, and does not incorporate information or assumptions about atmospheric transport or source regions. Given that the availability of multiple satellite data sets has already resulted in a research shift from modeling-only to observational-based assessments of aerosol forcing [*Yu et al.*, 2006], geostatistical data fusion can potentially provide useful optimal fused data sets, taking advantage of the strengths, and minimizing the limitations, of each individual sensor in a new way.

[9] The remainder of this paper is organized as follows. Section 2 provides a description of the MISR, MODIS and AERONET data used in the presented analysis. Section 3 gives an overview of the applied method and examined test cases. Results are presented and discussed in section 4. The code used to obtain the presented results is available from http://puorg.engin.umich.edu/code.php under the acronym of GDF AOT.

2. Data

[10] The description of the data sets presented here covers only the specific data products used in this study. The reader is referred to *Martonchik et al.* [2009] and L. A. Remer et al. (Algorithm for remote sensing of tropospheric aerosol from MODIS: Collection 005, Rev. 2, 2009, 97 pp., http://modis-atmos.gsfc.nasa.gov) for descriptions of the retrieval algorithms and *Yu et al.* [2006] for an overview of how tropospheric aerosols are measured. All analyses are performed using data from 2001.

2.1. AERONET

[11] AERONET is a globally distributed network of over 200 automated ground-based instruments covering all major tropospheric aerosol regimes [*Holben et al.*, 1998, 2001]. The instruments used are CIMEL sun/sky radiometers that make direct sun measurements with a 1.28° full field-of-view every 15 min in eight spectral bands [*Holben et al.*, 1998]. Level 2 (validated) AOT data are used here for 32 sites within the continental United States. The AERONET data archive (http://aeronet.gsfc.nasa.gov), includes AOT at different wavelengths, relative errors of AOT, Angstrom exponents (α) among different bands, and sampling dates and time. AERONET AOT measurements at 440 nm and 675 nm were interpolated to 555 nm to allow a straight-

forward comparison with the MISR and MODIS AOT products, using the methodology of *Liu et al.* [2004a],

$$\alpha_{\lambda_1-\lambda_2} = -\frac{\ln(\tau_{\lambda_1}/\tau_{\lambda_2})}{\ln(\lambda_1/\lambda_2)}, \quad (1)$$

where τ_{λ_1} and τ_{λ_2} are AOTs at wavelengths λ_1 and λ_2, respectively. The estimated standard deviation of the AERONET optical depth data errors is reported to be approximately 0.01 at wavelengths above 440 nm, and below 0.02 for shorter wavelengths [*Holben et al.*, 1998; *Eck et al.*, 1999].

2.2. MISR

[12] The MISR instrument aboard the Terra satellite has been providing continuous observations of AOT and aerosol type since late February 2000. These data are hosted at the Langley Research Centre Distributed Active Archive Centre (DAAC). The MISR data used in this study were obtained using the AMAPS system [*Paradise et al.*, 2010]. The green band (0.55 μm) RegBestEstimateSpectralOptDepth data field was extracted for the study area from the Level 2 aerosol product, version F09_0017 and later. The spatial resolution of the data set is 17.6 km. Theoretical sensitivity studies for MISR [*Kahn et al.*, 2001] have estimated the standard deviations of the measurement error associated with the optical depth to be 0.05 (or 0.2τ, whichever is larger) with a systematically tighter envelope over ocean than over bright land surfaces. About two thirds of MISR-AERONET coincidences fell within this envelope globally for the early post launch algorithm [*Kahn et al.*, 2005a].

2.3. MODIS

[13] The MODIS instrument is also aboard the Terra satellite. Terra Collection 005 Level-2 data at 0.55 μm were obtained using the AMAPS system. The "standard" aerosol product data field Corrected_Optical_Depth_Land was employed, which has a spatial resolution of 10 km and has been screened for quality 3 (QC = 3) over land. MODIS performs near-global daily observations of atmospheric aerosols, and can measure aerosol optical thickness with an error standard deviation of $0.05 + 0.15\tau$ over the land and $0.03 + 0.05\tau$ over the ocean [*Remer et al.*, 2005, 2008].

3. Methods

3.1. Comparison of MISR, MODIS, and AERONET Data

[14] Correlation coefficient analysis has been widely applied for comparing satellite retrievals with ground-based measurements [*Chu et al.*, 2002; *Liu et al.*, 2004a; *Abdou et al.*, 2005]. The goals of the analysis presented here are to characterize AOT differences between sensors by location and season. Correlation coefficients provide an assessment of the fraction of variance (i.e., variability) in the AERONET AOT that can be explained by the MISR and MODIS observations. In other words, this analysis assesses the degree to which the spatial and temporal variability of the MISR or MODIS observations are consistent with that of the AERONET data.

[15] The AOT data from the three sensors cannot be compared directly, in part because they are reported at different spatial resolutions. Therefore, following the methodology of *Liu et al.* [2004a], the mean of MISR and MODIS observations within a 0.5° by 0.5° bounding box around each AERONET site is used as a basis for comparison to AERONET data, which are themselves averaged over ±30 min from the Terra overpass. Correlation coefficients are used to characterize the agreement between daily data pairs from the 32 AERONET sites and the corresponding MISR or MODIS observations at those sites.

3.2. Investigation of the Spatial and Temporal Variability in MISR and MODIS AOT

[16] AOT varies spatially and temporally. This variability can be quantified using variogram analysis, a geostatistical spatial analysis tool. Although the AERONET network is too sparse to independently characterize the spatial variability at the continental scale, it can be used for regional analyses in areas when the network is relatively dense. On the other hand, the dense MISR and MODIS data coverage provides good information about AOT spatial variability as captured by these instruments. Analysis of the MISR and MODIS AOT spatial variability provides insights into differences in the way that these instruments capture the AOT distribution. Differences may be due to the differences in the observational spatial resolution and sampling, instrument signal-to-noise ratios, or retrieval algorithms.

[17] For assessing the AOT temporal variability, the AERONET network is the better candidate, due to its frequent temporal sampling during daylight hours, unlike the snapshots from MISR and MODIS. However, when the spatial and temporal variability is examined simultaneously, the MISR and MODIS AOT retrievals can also provide useful information about space-time variability. For simplicity, the spatial and temporal analysis is presented here using the MISR and MODIS data, but the conclusions about the temporal variability are consistent with those obtained using the AERONET observations (results not shown). The temporal component of the analysis is useful for identifying the time scales over which the AOT data can be integrated into relatively contiguous maps without introducing errors due to correlations in the temporal variability of the AOT.

[18] The spatiotemporal autocorrelation analysis is performed using variogram analysis [e.g., *Chiles and Delfiner*, 1999]. For all pairs of AOT data from a given instrument (e.g., MISR), the raw variogram is evaluated as

$$\gamma(h_x, h_t) = \frac{1}{2}\left[\left(z(x_i, t_i) - z(x_j, t_j)\right)^2\right], \quad (2)$$

where z are the AOT observations at locations x_i and x_j and times t_i and t_j, h_x is the spatial separation distance between the two observation locations, and h_t is the temporal lag in days between the observations. The distance h_x is calculated as the great circle distance between the locations x_i and x_j,

$$h_x(x_i, x_j) = r\cos^{-1}\left(\sin\phi_i \sin\phi_j + \cos\phi_i \cos\phi_j \cos(\theta_i - \theta_j)\right), \quad (3)$$

where (ϕ_i, θ_i) are the longitude and latitude of location x_i, and r is the Earth's mean radius. In the analysis presented here, a raw variogram is created for each repeat cycle of MODIS and MISR (i.e., each available 16 day period in 2001).

[19] Once the raw variograms are obtained, the variability can be visualized by binning the variances γ into preset ranges of separation distances (h_x) and time lags (h_t). The binned version of the raw variogram is referred to as the experimental variogram. If the temporal autocorrelation of the observations across multiple days is negligible, the experimental variogram can be presented as a function of spatial lag only, and a theoretical model can be selected to represent the observed spatial-only variability. In the analyses presented here, an exponential model was found to represent the spatial autocorrelation of the AOT data well,

$$\gamma_{theo}(h_x) = \begin{cases} 0 & h_x = 0 \\ \sigma_n^2 + \sigma_b^2\left(1 - \exp\left(-\frac{h_x}{l}\right)\right) & h_x > 0 \end{cases}, \quad (4)$$

where σ^2 ($= \sigma_n^2 + \sigma_b^2$) represents the variance of observed AOT at large separation distances (i.e., for uncorrelated observations) and l is the range parameter. The correlation length beyond which autocorrelation between points becomes negligible is defined as approximately $3l$ [e.g., *Chiles and Delfiner*, 1999]. The variance σ_n^2 is the nugget, representing both the measurement error and the small-scale variability at distances smaller than those resolved by available observations, whereas σ_b^2 represents the variance of the portion of the AOT variability that is spatially correlated. These parameters are optimized using a least squares fit to the spatial raw variogram. Conceptually, a higher variance is indicative of greater overall variability, and a shorter correlation length indicates greater spatial variability at smaller scales.

3.3. Geostatistical Data Fusion Approach

[20] Universal kriging [e.g., *Chiles and Delfiner*, 1999], a geostatistical data fusion approach, makes it possible to fuse auxiliary variables with full spatial coverage (e.g., MISR and MODIS AOT) to improve the interpolation of a primary data set with observations at a finite number of locations (e.g., AERONET AOT). The auxiliary variables fill a role analogous to regressors in multiple linear regression, but within a framework that accounts for the spatial autocorrelation of the estimated field, and can reproduce observed AERONET AOT measurements exactly at sampling locations.

[21] The objective is to estimate the AOT distribution ($\mathbf{s}$) at m locations and times (typically defined on a regular grid), given the AERONET AOT measurements at n locations and times, where $\mathbf{s}$ ($m \times 1$) is modeled as the sum of a deterministic but unknown component $\mathbf{X_s}\boldsymbol{\beta}$ (also known as the trend or drift), and a zero-mean stochastic component $\boldsymbol{\nu}$,

$$\mathbf{s} = \mathbf{X_s}\boldsymbol{\beta} + \boldsymbol{\nu}, \quad (5)$$

where $\mathbf{X_s}$ ($m \times p$) defines the model of the trend. $\boldsymbol{\beta}$ is a $p \times 1$ vector of drift coefficients that define the weights assigned to each of the p variables in the model of the trend, and are estimated as described in equation (11). Note that in the field of geostatistics, the trend or the drift refers to the component of spatial variability that can be represented as a deterministic function of other available variables. This is different from the fields of atmospheric and climate sciences where the term 'trend' typically refers to a net temporal change. For the case examined here, the model of the trend $\mathbf{X_s}$ includes a column of ones, which will multiply a $\boldsymbol{\beta}$ representing an overall constant or intercept, as well as columns with the MISR and MODIS AOT data sets at all estimation locations and times. Because AERONET, MISR, and MODIS all measure AOT, a linear relationship between the AERONET, and MISR and MODIS AOT is both the simplest and a reasonable model, yielding a linear model of the trend,

$$\mathbf{X_s} = \begin{bmatrix} 1 & MISR_{AOT_1} & MODIS_{AOT_1} \\ 1 & MISR_{AOT_2} & MODIS_{AOT_2} \\ \cdot & \cdot & \cdot \\ \cdot & \cdot & \cdot \\ 1 & MISR_{AOT_m} & MODIS_{AOT_m} \end{bmatrix}. \quad (6)$$

Analogous to a multiple regression model, the constant term is the first component of this linear model of the trend, and aims to capture a net offset or intercept (i.e., the mean of the portion of the AOT distribution that is not captured by MISR and MODIS). This constant term thereby also represents any systematic offset between the combined MISR and/or MODIS AOT and the AOT distribution as sampled by AERONET.

[22] At the AERONET locations, the stochastic component $\boldsymbol{\nu}$ in equation (5) represents the observed spatial and temporal residuals between the AERONET AOT measurements and the weighted MISR and MODIS AOT observations. At the estimation locations, this component represents the predicted residuals between the true AOT and the weighted MISR and MODIS AOT at those locations/times. The covariance of these residuals is described using a matrix $\mathbf{Q}$, where the covariance function is defined based on the variogram analysis (equation (4)), such that the covariance between two points x_i and x_j is defined as

$$Q_{ij} = \sigma^2 - \gamma_{theo}(h_x) = \begin{cases} \sigma_n^2 + \sigma_b^2 & h_x = 0 \\ \sigma_b^2 \exp\left(-\frac{h_x}{l}\right) & h_x > 0 \end{cases}. \quad (7)$$

In this case, the variogram analysis is carried out on the detrended AERONET AOT data ($\mathbf{z}$–$\mathbf{X_s}\boldsymbol{\beta}$) within the specific regions where universal kriging is applied. The detrending is carried out by subtracting the trend composed of the constant plus the MISR and MODIS AOT ($\mathbf{X_s}$) by their corresponding drift coefficients ($\boldsymbol{\beta}$, equation (11)) from the AERONET AOT. The analysis presented in section 4 focuses on regions where the AERONET network is sufficiently dense to estimate the spatial variability on regional scales using the AERONET data. The nugget (σ_n^2, equation (4)) in this case is found to be zero. Because the nugget represents both measurement error and microvariability, this indicates that the measurement error of AERONET AOT is negligible relative to the total amount of variability, which is consistent with the reported AERONET AOT precision of ±0.01, as described in section 2.1.

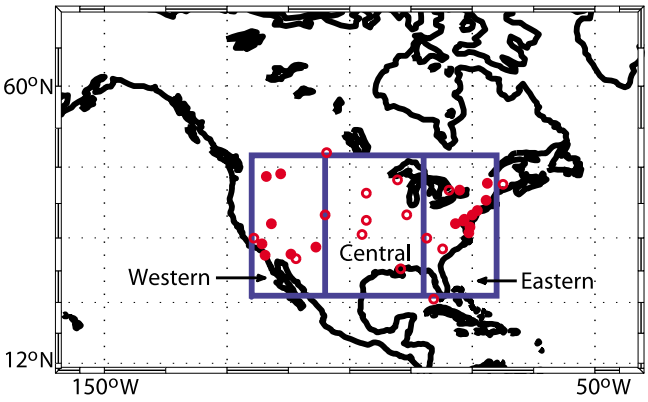

Figure 1. Location of AERONET sites used in the correlation analysis. The examined regions are outlined in blue. Solid circles represent observation locations also used in the universal kriging test cases.

[23] The estimates of AOT at the target times and locations are obtained by solving the linear system of universal kriging equations [e.g., *Chiles and Delfiner*, 1999],

$$\begin{bmatrix} \mathbf{Q_{zz}} & \mathbf{X_z} \\ \mathbf{X_z^T} & \mathbf{0} \end{bmatrix} \begin{bmatrix} \mathbf{\Lambda}^T \\ \mathbf{M} \end{bmatrix} = \begin{bmatrix} \mathbf{Q_{zs}} \\ \mathbf{X_s^T} \end{bmatrix}, \tag{8}$$

where $\mathbf{Q_{zz}}$ is the $n \times n$ spatial covariance matrix defined between AERONET observation locations based on equation (7), $\mathbf{X_z}$ ($n \times p$) is the model of the trend defined at the measurement locations based on equation (6), $\mathbf{Q_{zs}}$ ($n \times m$) represents the covariance evaluated between the measurement and the estimation locations again based on equation (7), and $\mathbf{X_s}$ ($m \times p$) is the model of the trend defined at the estimation locations again based on equation (6). When multiple time periods are used in the analysis, as is true for the test cases described in section 3.4, the correlation between time periods is assumed to be zero. The system of equations is solved for $\mathbf{M}$, a $p \times m$ matrix of Lagrange multipliers, and $\mathbf{\Lambda}$, the $m \times n$ matrix of weights to be assigned to AERONET AOT observations for interpolation to each of the m locations and times,

$$\hat{\mathbf{s}} = \mathbf{\Lambda z}, \tag{9}$$

where $\hat{\mathbf{s}}$ is the final AOT estimate at m locations/times that include information derived from all three sensors, and $\mathbf{z}$ are the n AERONET observations. The covariance matrix defining the uncertainty associated with these estimates is:

$$\mathbf{V_{\hat{s}}} = \mathbf{Q_{ss}} - \mathbf{\Lambda}^T\mathbf{Q_{zs}} - \mathbf{X_s M}, \tag{10}$$

where the diagonal elements of $\mathbf{V_{\hat{s}}}$ represent the predicted error variance ($\sigma^2_{\hat{\mathbf{s}}}$) of individual elements in $\hat{\mathbf{s}}$, i.e., of the estimates of AOT at individual locations and times. Finally, the influence of MISR and MODIS on the final estimates $\hat{\mathbf{s}}$ can be quantified by calculating the estimated drift coefficients $\boldsymbol{\beta}$ ($p \times 1$) and their corresponding uncertainties for these two data sets:

$$\hat{\boldsymbol{\beta}} = \left(\mathbf{X_z^T Q_{zz}^{-1} X_z}\right)^{-1} \mathbf{X_z^T Q_{zz}^{-1} z} \tag{11}$$

$$\mathbf{V}_{\hat{\boldsymbol{\beta}}} = \left(\mathbf{X_z^T Q_{zz}^{-1} X_z}\right)^{-1}, \tag{12}$$

where the diagonal elements of $\mathbf{V}_{\hat{\boldsymbol{\beta}}}$ represent the uncertainty of the individual drift parameters ($\sigma^2_{\hat{\boldsymbol{\beta}}}$), and the off-diagonal terms represent the estimated covariance of the errors associated with these estimates.

[24] Using these drift coefficients, the estimated AOT field in equation (9) can also be expressed as

$$\hat{\mathbf{s}} = \mathbf{X_s}\hat{\boldsymbol{\beta}} + \mathbf{Q_{zs}^T Q_{zz}^{-1}}\left(\mathbf{z} - \mathbf{X_z}\hat{\boldsymbol{\beta}}\right). \tag{13}$$

Comparing the estimated drift coefficients ($\hat{\boldsymbol{\beta}}$) and their uncertainties ($\sigma_{\hat{\boldsymbol{\beta}}}$) for MISR and MODIS observations gives an indication of which of the satellite observations contributes more strongly to the estimated AOT. The significance of the contribution of each set of observations can be assessed by calculating the coefficient of variation of its drift coefficient ($\sigma_{\hat{\boldsymbol{\beta}}}/\hat{\boldsymbol{\beta}}$). A coefficient of variation below 0.5 implies a statistically significant contribution to the estimated trend at the 0.05 (i.e., $2\sigma_{\hat{\boldsymbol{\beta}}}$) significance level.

[25] Recall that the drift coefficients are the weights assigned to the MISR and MODIS AOT data sets. These weights remain constant over the domain of analysis. As a consequence, the relationship between the true (as represented by AERONET) AOT, and MISR and MODIS AOT, is implicitly assumed to remain constant within an examined region. This is one of the reasons for which the test cases examined in section 3.4 are conducted regionally, because the relationship between MISR, MODIS, and AERONET cannot necessarily be assumed to remain constant throughout the continental United States.

[26] Ordinary kriging, a simple geostatistical interpolation technique, is used for comparison to the universal kriging estimates in the presented analyses. Ordinary kriging is one of the most commonly used techniques in geostatistical gap filling, but it lacks the advantage of using information from multiple sensors. In the ordinary kriging approach, the model of the trend is defined as $\mathbf{X_s} = [1 \ldots 1]^T$, and the covariance is derived using a variogram of the AERONET observations without detrending. The other equations remain unchanged. Past applications of ordinary kriging in aerosol science have been limited to the estimation of aerosol species over various regions [*Zapletal*, 2001; *Delalieux et al.*, 2006], and have not been aimed at comparison with other estimation techniques. In this work, because the true AOT distribution is unknown, the ordinary kriging estimates are used as a baseline for evaluating the estimates from universal kriging. By comparing the two kriging estimates, we identify the effect of using additional satellite observations on both the AOT estimates and the uncertainty associated with those estimates.

3.4. Test Cases

[27] The correlation analysis (section 3.1) is carried out for three regions over the contiguous United States for selected periods in 2001. Recognizing that aerosol distributions can be both site and season specific, the United States are divided into three regions (Western, Central, and Eastern), as illustrated in Figure 1. In the Western region, we expect dust to be dominant, along with biomass burning during the summer and autumn months. Biogenic aerosols often dominate the southeast, especially in summer, where biomass burning may also be important in some seasons.

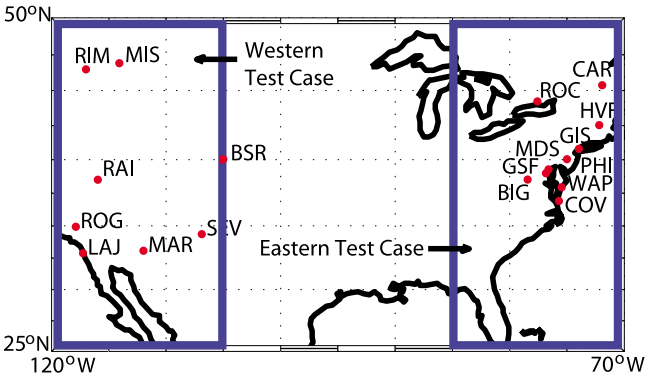

Figure 2. AERONET sites used for the Western and Eastern test cases. The AERONET sites in the Western region are Missoula (MIS), Rimrock (RIM), BSRN-BAO-Boulder (BSR), Railroad Valley (RAI), Rogers Dry Lake (ROG), La Jolla (LAJ), Maricopa (MAR), and Sevilleta (SEV); the AERONET sites in the Eastern region are Rochester (ROC), Cartel (CAR), Harvard Forest (HVF), GISS (GIS), Philadelphia (PHI), MD Science Centre (MDS), GSFC (GSF), Big Meadows (BIG), Wallops (WAP), and Cove (COV).

Four seasons are considered: Winter (DJF), Spring (MAM), Summer (JJA) and Fall (SON). Following previous studies [*Kahn et al.*, 2005a; *Liu et al.*, 2004a; *Abdou et al.*, 2005], the correlation analysis was carried out at a daily scale.

[28] The spatiotemporal analysis is carried out using the MISR and MODIS data sets. The analysis is performed at the native resolution of MISR (i.e., 17.6 km) and MODIS (i.e., 10 km) AOT for each 16 day repeat cycle of the Terra satellite in 2001. By doing this analysis for each 16 day repeat cycle, the seasonal changes in spatiotemporal variability of AOT can be assessed, as well as how these changes relate to the periodic changes in the underlying AOT processes over the continental United States.

[29] Finally, the geostatistical data fusion analysis is presented using two test cases, the first being over the Eastern United States during autumn, and the second over the Western United States during summer (Figure 2). Table 1 outlines the details of these two test cases. For these test cases, the study region is broken up into 0.2° × 0.2° grid cells at which the AOT estimates are obtained. The MISR and MODIS observations used for this analysis are averages of all the MISR and MODIS AOT observations falling within a given 0.2° × 0.2° grid cell. This particular estimation resolution was chosen to show the flexibility of the universal kriging approach in estimating AOT at very fine resolutions, but in general could be performed at coarser estimation scales as well.

[30] As will be shown in section 4.2, there is little significant temporal autocorrelation in the day-to-day variability in the MISR and MODIS AOT within a 7 day period. As a result, the geostatistical data fusion is performed in 1 week increments, using weekly averaged AOT data from AERONET, MISR and MODIS. These averaged AOT data are used to obtain estimates of the average spatial distribution of AOT over those 7 day periods. For each 7 day period, AERONET sites that have AOT data for at least 3 of the 7 days, and which have overlapping MISR and MODIS data, are used in the analysis. As a result, for the Eastern Test Case during autumn, two to ten sites are used during the various weeks, whereas for the Western Test Case during summer, two to eight sites are used in each week. Figure 2 shows the locations of all the sites used in the test cases. It should be noted here that there may be cases in which significant temporal autocorrelation may exist (e.g., near sources) where shorter time scale variations are predominant, or where strong gradients occur in transported aerosols. In such cases the data fusion approach should be applied with caution.

[31] The AOT estimates obtained from universal kriging (henceforth denoted as AOT_{UK}) are compared with AOT estimates obtained from ordinary kriging (henceforth denoted as AOT_{OK}). Cross validation is used to compare the two estimates. In this approach, individual AERONET 7 day observations at a given site are sequentially eliminated from the analysis, and estimates at these locations and times are obtained using the remaining AERONET observations, and, for AOT_{UK}, using available MISR and MODIS data as well. Because AERONET measurements have traditionally been used for validating satellite observations of MISR and MODIS [*Kahn et al.*, 2005a; *Remer et al.*, 2005; *Yu et al.*, 2006], the withheld AERONET observations are used to evaluate the relative precision and accuracy of the AOT_{OK} and AOT_{UK} estimates.

[32] The evaluation of AOT_{OK} and AOT_{UK} estimates is carried out using three metrics. First, the root mean square error (RMSE) is calculated between the estimated AOT and the AERONET observations. Second, the magnitude of the predicted kriging uncertainties is evaluated by calculating the root mean square prediction error (RMSPE) of the kriging uncertainties (equation (10)). Third, the accuracy of these predicted uncertainties is evaluated by verifying the percent of true AERONET AOT observations that fall within two standard deviations of the estimated AOT, where the standard deviations are those predicted by the kriging analyses (equation (10)). This third metric is less sensitive to extreme outliers, and, in an ideal scenario, 95% of the true AOT should fall within this interval. Values significantly below 95% would indicate an underestimation of the true uncertainties, while values substantially above 95% indicate overly conservative estimates. All three metrics are calculated across the entire season for both test cases.

Table 1. Test Case Specifications

Test Case	Time Period	Spatial Extent	Estimation Resolution		Number of AERONET Locations
			Spatial	Temporal	
Eastern	Fall	70°W-85°W 25°N-50°N	0.2° × 0.2°	Average over a 7 day period	10
Western	Summer	105°W-120°W 25°N-50°N	0.2° × 0.2°	Average over a 7 day period	8

Table 2. Correlation Coefficients Between AERONET Measurements and MISR and MODIS Observations Classified by Region (Figure 1) and Season for the Year 2001[a]

	Winter (DJF)		Spring (MAM)		Summer (JJA)		Fall (SON)		All Months	
	MISR	MODIS	MISR	MODIS	MISR	MODIS	MISR	MODIS	MISR	MODIS
Western	*0.49*	*0.09*	**0.67**	*0.29*	*0.47*	*0.32*	**0.59**	*0.09*	**0.63**	*0.30*
Central	***0.92***	**0.51**	**0.68**	**0.61**	**0.73**	**0.58**	**0.67**	*0.43*	***0.80***	**0.59**
Eastern	***0.79***	**0.70**	**0.52**	***0.77***	***0.86***	***0.87***	***0.82***	***0.80***	***0.78***	***0.84***

[a]Low correlation coefficient (0–0.5) cases are in italics, medium correlation coefficient (0.5–0.75) cases are boldface, and high correlation coefficient cases (0.75–1.00) are italic boldface. The lowest correlations occur in the west, where bright surfaces and mixtures of spherical particles and nonspherical dust dominate, and in the winter months, when total-column AOT tends to be low, and AOT is near the sensitivity limit of the satellite instruments. DJF, December–February; MAM, March–May; JJA, June–August; SON, September–November.

[33] Overall, the two examined test cases are designed to (1) demonstrate the versatility of the universal kriging technique in estimating AOT over different regions and across seasons and (2) evaluate the improvement of universal kriging estimates over ordinary kriging estimates (or simply the AOT fields observed by MISR or MODIS individually) as a function of the strength of the relationship between MISR, MODIS, and AERONET AOT.

4. Results and Discussion

4.1. Comparison of MISR, MODIS, and AERONET Data Sets

[34] The results of the correlation analysis are presented in Table 2, and reveal that MISR data have a stronger correlation to AERONET data ($0.47 < \rho < 0.92$) than do MODIS data ($0.09 < \rho < 0.61$) across seasons in the Western and Central regions. Given that the correlation coefficient is an indication of the degree of linear covariability between the data sets, this implies that MISR is better able to explain the variability in the AERONET AOT than MODIS over these regions. Note that for MODIS, the "standard" product was used in this paper, and it is plausible that using the more recent "Deep Blue" product, which was not available at the time of analysis, would have shown better agreement with the AERONET AOT, at least over bright surfaces. On the other hand, the particle properties used in the MODIS standard AOT retrieval over land are assumed based on AERONET values [*Levy et al.*, 2007], whereas for MISR, particle properties are retrieved along with AOT as part of a self-consistent process [*Martonchik et al.*, 2009].

[35] The weak correlation in the Western region for both instruments is primarily due to low AOT values in this region, which are near the lower limit of retrieval sensitivity for MISR and MODIS. *Liu et al.* [2004a] points out that low values of AOT, as well as coarse-particle dominated scenarios, may produce poor correlations with AERONET AOT. This does not necessarily indicate poor MISR or MODIS performance; rather, at very low AOT values, the correlation coefficients are not informative because the uncertainty associated with the satellite retrievals is large compared to the magnitude of the AOT itself. The high surface albedo in the Western sector and the frequent atmospheric loading with nonspherical mineral dust are additional obstacles to obtaining good satellite retrievals of AOT over this region.

[36] In the Eastern region, the MISR ($0.52 < \rho < 0.86$) and MODIS ($0.70 < \rho < 0.87$) data show comparable correlations to AERONET across seasons, and are able to capture the AERONET AOT variability better than across the other two examined regions. The year-round correlation coefficients ($\rho = 0.78$ for MISR and $\rho = 0.84$ for MODIS) are similar to values that have been reported previously for continental sites in this region [*Chu et al.*, 2002; *Liu et al.*, 2004a; *Kahn et al.*, 2005a].

[37] Overall, results from this analysis are consistent with previous findings that indicate that differences between MISR and MODIS AOT relative to AERONET AOT are caused by site-specific effects and aerosol-size-distribution effects.

[38] This initial analysis indicates that the information provided by MISR and MODIS with regard to the AOT distribution as measured by the AERONET network varies regionally and seasonally throughout the continental United States. Based on these results, it is expected that the universal kriging analysis should outperform ordinary kriging in the Eastern region, where the correlations between the AERONET data and the MISR and MODIS data are strong. In other regions, the additional information provided by MODIS and MISR is less significant, and the universal kriging and ordinary kriging analyses are expected to be more similar to one another.

4.2. Spatiotemporal Variability Analysis

[39] The spatiotemporal variability analysis is performed for MISR and MODIS AOT for each 16 day repeat cycle in 2001 for the Terra satellite. For each repeat cycle, a spatiotemporal experimental variogram is obtained. Example variograms are presented for MISR and MODIS in Figures 3a and 3b, for 11 to 26 April 2001. These variograms represent the expected variance of pairs of MISR (Figure 3a) or MODIS (Figure 3b) observations, separated by a given distance in space and time lag.

[40] Figures 3a and 3b do not exhibit any noticeable temporal autocorrelation in the day-to-day variability of the AOT distribution for time lags up to 7 days. The temporal lag (shown on the vertical axis) in Figures 3a and 3b represents the number of days between the times when two observations are recorded. A temporal lag of 1 day could therefore represent, for example, the expected variance between observations taken on days 14 and 15, or on days 1 and 2 of the repeat cycle. The lack of temporal correlation indicates that the coherent temporal variability in the AOT takes place either at subdiurnal scales that cannot be captured by the examined remote sensing data products, and/or at longer time scales, potentially representative of seasonal variability.

[41] Since the results of this analysis indicate that temporal correlation is not significant for time lags up to 7 days,

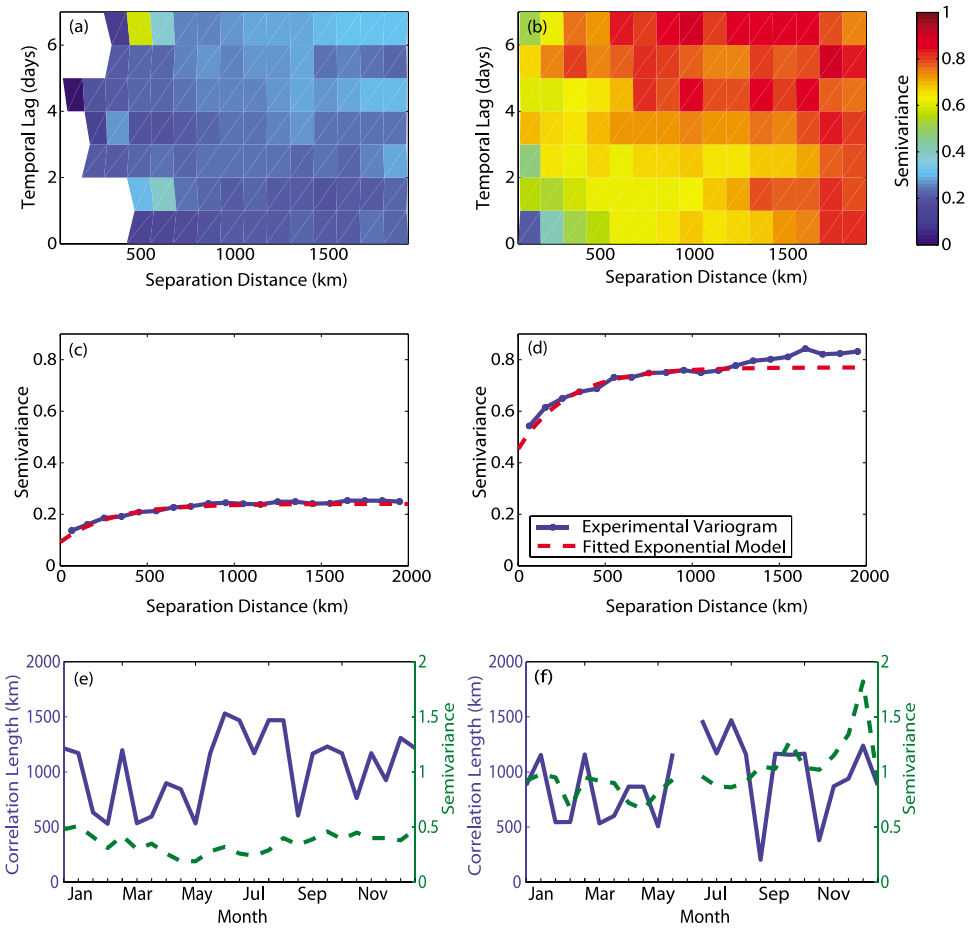

Figure 3. Spatial and temporal variograms of AOT over a 16 day period from April 11 to April 26, 2001 for (a) MISR and (b) MODIS. The color bar indicates the semivariance. Spatial variogram over the same period from (c) MISR and (d) MODIS, using all data over the 16 day period. Correlation length ($3l$) and variance (σ^2) of AOT for all 16 day periods in 2001 for (e) MISR and (f) MODIS. Note that MODIS had no data for one repeat cycle in June.

MISR and MODIS data taken over a week can be integrated into a single map. In other words, multiple days of data can be used concurrently to inform the data fusion analysis. Note that the lack of temporal autocorrelation does not necessarily imply a lack of temporal variability, but simply that the observed AOT is not correlated from day to day.

[42] On the other hand, Figures 3a and 3b reveal that the MISR and MODIS AOT data do exhibit strong spatial autocorrelation, as evidenced by the fact that the variance increases as the spatial separation distance increases. This is more clearly visible in Figures 3c and 3d, where all data from the 11 to 26 April repeat cycle are examined in a single spatial variogram. Figures 3c and 3d display both the experimental and the fitted theoretical spatial variograms for MISR and MODIS. They indicate that the correlation length of AOT data (i.e., the lag distance at which the semivariance reaches an asymptote) is approximately 900 km for both instruments for the examined time period, indicating that observations separated by longer distances are essentially independent.

[43] Figures 3e and 3f present the parameters of the fitted theoretical spatial variograms for each of the 25 Terra repeat cycles in 2001. This analysis shows that the spatial autocorrelation of the MISR and MODIS AOT data are quite consistent with one another (blue lines in Figures 3e and 3f). The correlation lengths vary significantly throughout the year, ranging from 500 km to 1500 km, with higher values prevalent during the summer months. On the other hand, the total amount of variability (i.e., variance) of the MODIS AOT is always significantly higher than that of MISR. During the winter months, both MISR and MODIS show shorter correlation lengths and increased variance, representative of a more heterogeneous distribution of aerosols. In general, the long-range transport of dust in late spring and summer, and smoke from summer through early autumn, are likely to contribute to the longer correlation lengths during the summer months, whereas local aerosol sources explain the smaller-scale variability observed during other seasons.

[44] Seasonal changes in the spatial variability of AOT will impact the uncertainty estimates obtained from universal kriging. During the summer months, due to the longer correlation lengths and smaller variance, the AOT estimates will have lower uncertainty, while, conversely, during the winter months, we expect higher estimation uncertainties.

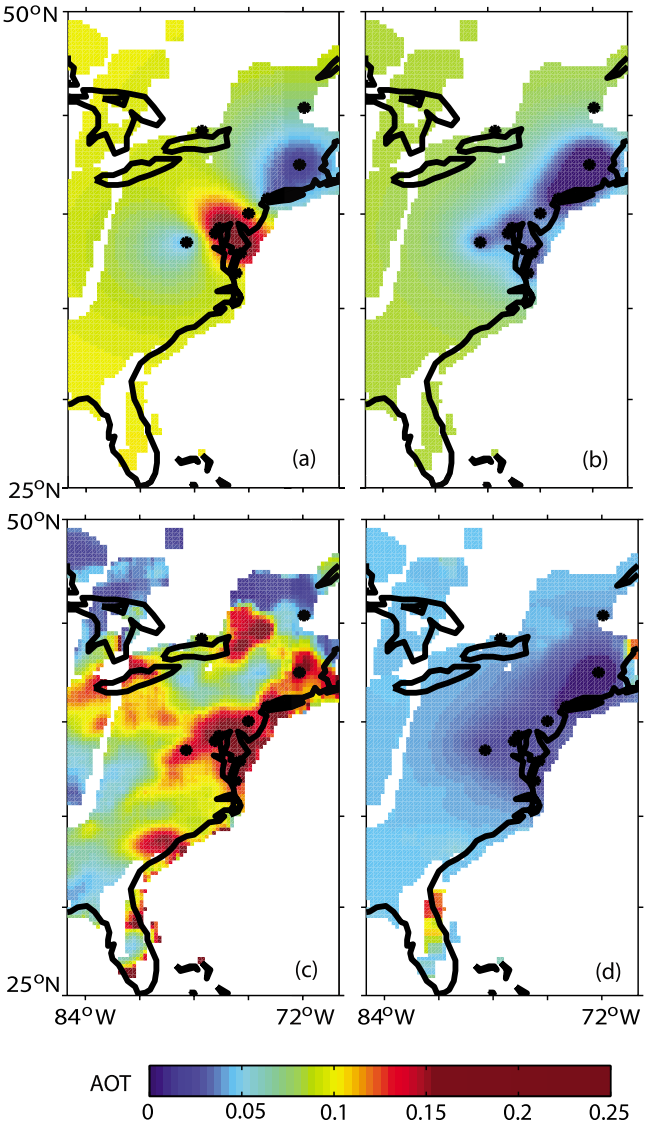

Figure 4. Comparison of AOT_{OK} with AOT_{UK} for Eastern test case for one period from 29 October to 4 November. The black asterisks indicate the locations of the AERONET sites. The white gaps indicate the 7 day satellite coverage mask that is imposed on both universal and ordinary kriging for ease of comparison. (a) Best estimates obtained from ordinary kriging. (b) Uncertainty associated with the ordinary kriging estimates, expressed as a standard deviation. (c) Best estimates obtained from universal kriging. (d) Uncertainty associated with the universal kriging estimates, expressed as a standard deviation.

[45] One interesting conclusion from Figure 3 is that the MODIS AOT variance is higher than that for MISR, across all seasons. This is due in part to the fact that the more frequent and finer-scale MODIS sampling captures more small-scale AOT variability than MISR. The second reason for this higher variance is that, due to its exclusively near-nadir viewing geometry, MODIS has a greater sensitivity to variability in surface brightness on small spatial scales, which in turn introduces some additional variability into the MODIS AOT retrievals. Neither of these features hinders the application of the universal kriging approach presented in this work. However, it has implications for researchers pursuing assimilation of MISR and MODIS radiance data, or looking to improve the retrieval algorithms of these two sensors.

4.3. Data Fusion Results

[46] Figures 4 and 5 show the estimated AOT field for 1 week for each of the case studies described in Table 1. The Eastern test case demonstrates that the universal kriging AOT estimates are better than the ordinary kriging estimates when MISR and MODIS are significantly correlated with the AERONET AOT observations. The associated uncertainties for the AOT_{UK} estimates are significantly lower. Cross validation at the AERONET locations confirms that the AOT_{UK} estimates are more realistic than the AOT_{OK} estimates, as shown for one of the 7 day periods in Figure 6 (see Figures S1 and S2 in the auxiliary material for the entire season).[1] Overall, for this test case, the RMSE for AOT_{UK} is 0.053, which is lower than that of AOT_{OK} (0.067) and each of the individual satellite data sets (0.054 for MISR and 0.056 for MODIS). The true AOT falls within the 2 standard deviations of both the kriging estimates for 93% of AERONET observations, but the RMSPE of AOT_{UK} (RMSPE = 0.035) is significantly lower than that of AOT_{OK} (RMSPE = 0.069). These results confirm that, when strong correlation exists between multiple data sets, the universal kriging approach can be used to obtain better predictions with smaller uncertainties relative to estimates based on measurements from a single sensor. This is evident not only from the reduction in uncertainty, but also from the lower RMSE and RMSPE values of AOT_{UK} relative to AOT_{OK}.

[47] The Western test case demonstrates that the universal kriging estimates are comparable to the ordinary kriging estimates in regions where the correlation with MISR and MODIS is low. The predicted uncertainty (Figure 5b and 5d) is similar for the two methods. This is consistent with our findings from the correlation analysis because MISR and MODIS are not strongly correlated with the AERONET AOT in this region (Table 2), and are therefore unable to capture the AERONET AOT variability. Cross-validation results shown in Figure 7 confirm that the two approaches provide similar estimates with high uncertainty (see Figure S3 and S4 in the auxiliary material for the entire season). The AERONET, MISR and MODIS AOT values are also plotted in Figure 7, and demonstrate that, for the examined case, both ordinary and universal kriging do better than using the MISR and MODIS data sets individually. This is further validated by the metrics calculated for the entire season. The RMSE for AOT_{UK} and AOT_{OK} is 0.047 and 0.048, respectively, which is lower than the RMSE of 0.082 for MISR and 0.260 for MODIS. The true AERONET AOT fall within 2 standard deviations of AOT_{UK} and AOT_{OK} estimates for 98% of available observations. Finally, the RMSPEs are similar for the ordinary (RMSPE = 0.066) and universal (RMSPE = 0.061) kriging approaches, reaffirming their similarity to one another for this test case.

[1] Auxiliary materials are available in the HTML. doi:10.1029/2009JD013765.

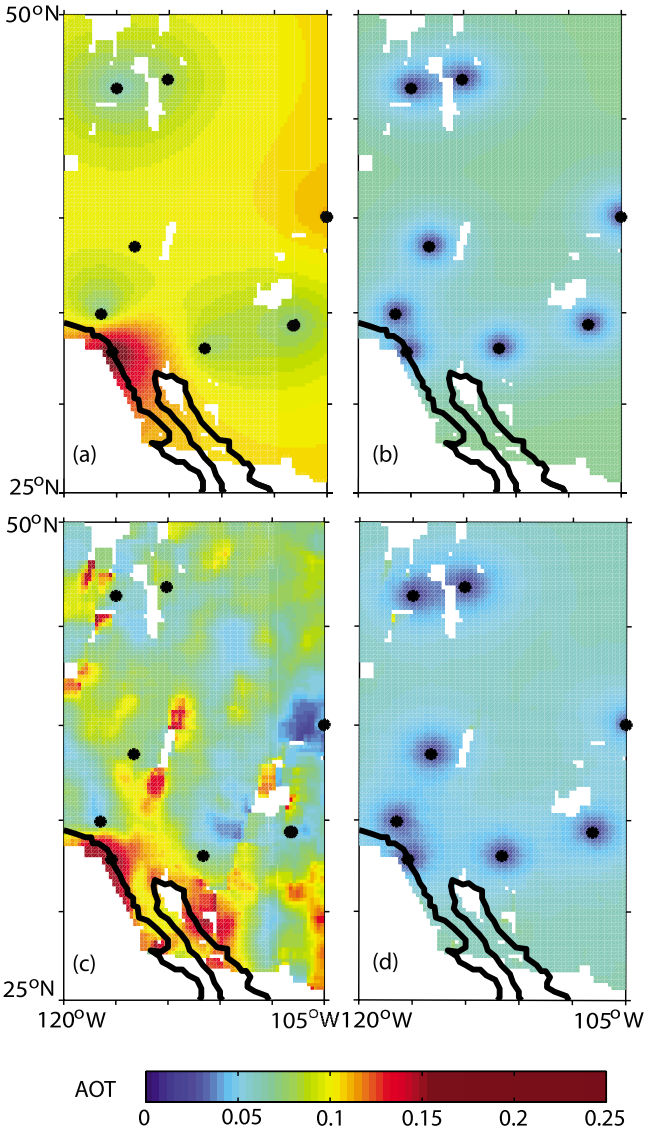

Figure 5. Comparison of AOT_{OK} with AOT_{UK} for Western test case for a 7 day period from 21 to 27 July. The black asterisks indicate the locations of the AERONET sites. The white gaps indicate the 7 day satellite coverage mask that is imposed on both universal and ordinary kriging for ease of comparison. (a) Best estimates obtained from ordinary kriging. (b) Uncertainty associated with the ordinary kriging estimates, expressed as a standard deviation. (c) Best estimates obtained from universal kriging. (d) Uncertainty associated with the universal kriging estimates, expressed as a standard deviation.

[48] In addition to predicting AOT, the universal kriging approach can be used to quantify which of the satellite observations has more influence on the estimation procedure, by looking at the drift coefficient ($\hat{\boldsymbol{\beta}}$) values, their uncertainties ($\sigma_{\hat{\beta}}$), and the corresponding coefficients of variation ($\sigma_{\hat{\beta}} / \hat{\boldsymbol{\beta}}$), as shown in Table 3. For the Eastern Test Case, the MODIS AOT observations have a more significant drift coefficient ($\sigma_{\hat{\beta}_2} / \hat{\beta}_2 = 0.18$) than the MISR data, and these latter data are therefore used primarily to adjust the spatial pattern in

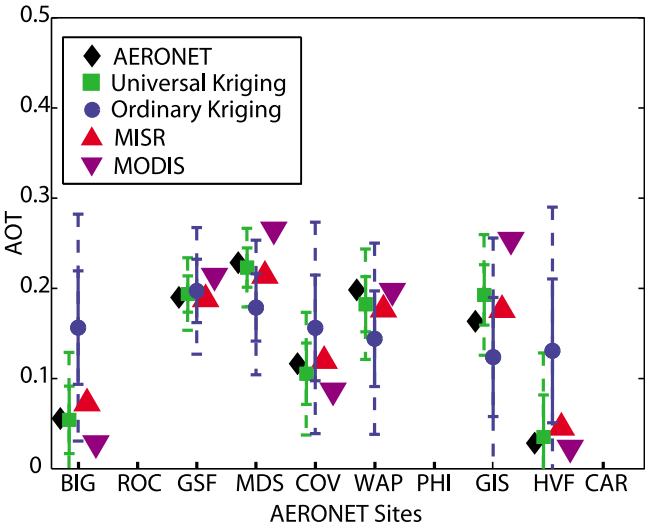

Figure 6. Cross-validation results for 29 October to 4 November for Eastern test case. Error bars represent $1\sigma_{\hat{s}}$ and $2\sigma_{\hat{s}}$ uncertainty bounds.

MODIS AOT to more closely resemble the AERONET AOT observations. Conversely, for the Western Test Case, the MISR AOT observations seem to be a significant predictor of AERONET AOT measurements ($\sigma_{\hat{\beta}_1} / \hat{\beta}_1 = 0.43$). In addition, the drift coefficient values for the constant term ($\hat{\beta}_0$) are not significantly different from zero for either examined case, indicating an absence of any systematic offset between the AOT predicted by the weighted combination of MISR and MODIS, and the AOT observed by AERONET.

[49] Finally, although this analysis used both MISR and MODIS in the data fusion process, one could easily use either MISR or MODIS individually, or some other AOT product(s). The approach presented combines the best

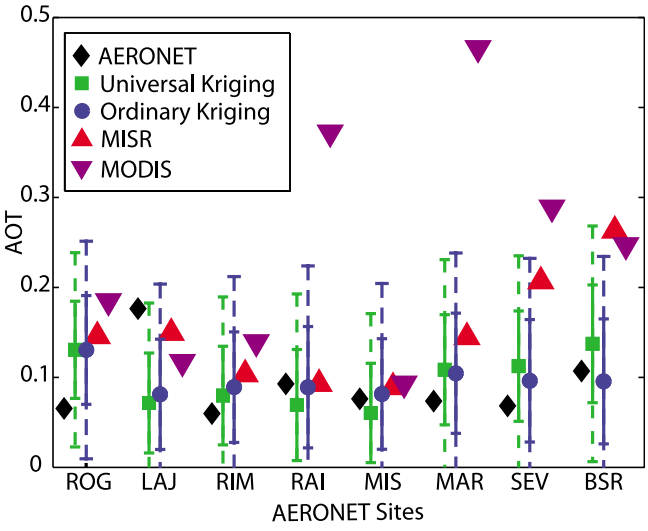

Figure 7. Cross-validation results for 21–27 July for Western test case. Error bars represent $1\sigma_{\hat{s}}$ and $2\sigma_{\hat{s}}$ uncertainty bounds.

Table 3. Drift Coefficient Values, Their Associated Uncertainties, and the Coefficient of Variation for the Two Test Cases From the Universal Kriging Model

	Constant			MISR			MODIS		
Test Case	$\hat{\beta}_0$	$\sigma_{\hat{\beta}_0}$	$\sigma_{\hat{\beta}_0}/\hat{\beta}_0$	$\hat{\beta}_1$	$\sigma_{\hat{\beta}_1}$	$\sigma_{\hat{\beta}_1}/\hat{\beta}_1$	$\hat{\beta}_2$	$\sigma_{\hat{\beta}_2}$	$\sigma_{\hat{\beta}_2}/\hat{\beta}_2$
Eastern	0.010	0.014	1.4	0.017	0.16	9.42	0.68	0.12	0.18
Western	0.027	0.024	0.88	0.37	0.16	0.43	0.040	0.070	1.75

available information from all available sensors to identify the optimal representation of the AOT distribution.

5. Conclusions

[50] A geostatistical data fusion technique is implemented for combining remote-sensing and ground-based observations of AOT. Results show that adopting the universal kriging approach based on the combination of MISR, MODIS and AERONET enables better estimation of AOT with reduced uncertainties, relative to estimates based on observations from a single instrument.

[51] All three examined data sets were found to display strong spatial autocorrelation in their measured AOT distributions. Although the total degree of AOT variability differed between MISR and MODIS, the spatial scales of this variability were similar for these instruments. The day-to-day temporal autocorrelation in MISR or MODIS AOT observations was found to be minimal, due at least in part to limited temporal sampling, making it possible to integrate such observations over multiple days to better infer the spatial distribution of AOT.

[52] As an increasing number of remote sensing observations become available, data fusion approaches such as the one presented here may hold the key to furthering our understanding of atmospheric aerosols. Although differences between instruments are always present, the approach implemented here takes advantage of their complementary features by combining the three data sets in a manner that is statistically robust. The approach relies on the availability of auxiliary variables (MISR and MODIS AOT, in the presented analysis) at all locations where the AOT is to be estimated, and assumed that the relationship between these auxiliary variables and the primary observations (AERONET AOT, in the presented analysis) remains constant throughout the examined region.

[53] Finally, this study reinforces the complementary value of remote-sensing and ground-based observations of AOT. Long-term monitoring of aerosol distributions is possible via remote sensing measurements, and these can be used to capture the spatiotemporal distribution of aerosols. Expected refinements in retrieval algorithms and sensor capabilities will improve the accuracy of the retrieved AOT further. By fusing these measurements with ground-based observations using techniques such as the one presented here, it will be possible to obtain reliable long-term estimates of AOT at national and even global scales.

[54] **Acknowledgments.** We thank our colleagues on the Jet Propulsion Laboratory's AMAPS system team for providing us with the MISR and MODIS data sets as well as Charles Antonelli for making the codes publicly available. We also specially thank three anonymous reviewers and Angela Benedetti for providing us with excellent suggestions and feedback. The authors would also like to thank the AERONET principal investigators for collecting the aerosol data over the United States. The University of Michigan component of this research was funded through the Jet Propulsion Laboratory's Director's Research and Development Fund under a contract with the National Aeronautics and the Space Administration. Additional support was provided through NASA grant NNX08AJ92G. The work of Ralph Kahn was supported in part by NASA's Climate and Radiation Research and Analysis Program, under H. Maring, NASA's Atmospheric Composition Program, and the EOS-MISR project.

References

Abdou, W. A., D. J. Diner, J. V. Martonchik, C. J. Bruegge, R. A. Kahn, B. J. Gaitley, K. A. Crean, L. A. Remer, and B. Holben (2005), Comparison of coincident Multiangle Imaging Spectroradiometer and Moderate Resolution Imaging Spectro-radiometer aerosol optical depths over land and ocean scenes containing Aerosol Robotic Network sites, *J. Geophys. Res.*, *110*, D10S07, doi:10.1029/2004JD004693.

Acker, J., and G. Leptoukh (2007), Online analysis enhances use of NASA Earth science data, *Eos Trans. AGU*, *88*(2), 14–17, doi:10.1029/2007EO020003.

Andreae, M. O. (1995), Climatic effects of changing atmospheric aerosol levels, in *World Survey of Climatology*, vol. 16, *Future Climates of the World*, edited by A. Henderson-Sellers, pp. 341–392, Elsevier, Amsterdam.

Andreae, M. O., et al. (1986), External mixture of sea salt, silicates, and excess sulfate in marine aerosols, *Science*, *232*, 1620–1623, doi:10.1126/science.232.4758.1620.

Chen, W.-T., R. Kahn, D. Nelson, K. Yau, and J. Seinfeld (2008), Sensitivity of multi-angle imaging to optical and microphysical properties of biomass burning aerosols, *J. Geophys. Res.*, *113*, D10203, doi:10.1029/2007JD009414.

Chiles, J.-P., and P. Delfiner (1999), *Geostatistics: Modeling Spatial Uncertainty*, Wiley-Intersci., Hoboken, N. J.

Chu, D. A., Y. J. Kaufman, C. Ichoku, L. A. Remer, D. Tanré, and B. N. Holben (2002), Validation of MODIS aerosol optical depth retrieval over land, *Geophys. Res. Lett.*, *29*(12), 8007, doi:10.1029/2001GL013205.

Delalieux, F., R. van Grieken, and J. H. Potgieter (2006), Distribution of atmospheric marine salt depositions over continental western Europe, *Mar. Pollut. Bull.*, *52*(6), 606–611, doi:10.1016/j.marpolbul.2005.08.018.

Diner, D. J., J. C. Beckert, T. H. Reilly, C. J. Bruegge, J. E. Conel, and R. A. Kahn (1998), Multi-angle imaging spectroradiometer (MISR) instrument description and experiment overview, *IEEE Trans. Geosci. Remote Sens.*, *36*, 1072–1087, doi:10.1109/36.700992.

Eck, T. F., B. Holben, J. Reid, O. Dubovik, A. Smirnov, N. T. O'Neill, I. Slutsker, and S. Kinne (1999), Wavelength dependence of the optical depth of biomass burning, urban, and desert aerosols, *J. Geophys. Res.*, *104*(D24), 31,333–31,349, doi:10.1029/1999JD900923.

Gupta, P., F. Patadia, and S. A. Christopher (2008), Multisensor data product fusion for aerosol research, *IEEE Trans. Geosci. Remote Sens.*, *46*, 1407–1415, doi:10.1109/TGRS.2008.916087.

Holben, B. N., et al. (1998), AERONET–A federated instrument network and data archive for aerosol characterization, *Remote Sens. Environ.*, *66*(1), 1–16, doi:10.1016/S0034-4257(98)00031-5.

Holben, B. N., et al. (2001), An emerging ground-based aerosol climatology: Aerosol optical depth from AERONET, *J. Geophys. Res.*, *106*(D11), 12,067–12,097, doi:10.1029/2001JD900014.

Intergovernmental Panel on Climate Change (IPCC) (2007), *Intergovernmental Panel on Climate Change Fourth Assessment Report, Working Group I Report: The Physical Science Basis*, edited by S. Solomon et al., Cambridge Univ. Press, Cambridge, U. K.

Jiang, X., Y. Liu, B. Yu, and M. Jiang (2007), Comparison of MISR aerosol optical thickness with AERONET measurements in Beijing metropolitan area, *Remote Sens. Environ.*, *107*(1–2), 45–53, doi:10.1016/j.rse.2006.06.022.

Kahn, R. A., P. Banerjee, and D. McDonald (2001), The sensitivity of multiangle imaging to natural mixtures of aerosols over ocean, *J. Geophys. Res.*, *106*(D16), 18,219–18,238, doi:10.1029/2000JD900497.

Kahn, R. A., B. Gaitley, J. Martonchik, D. Diner, K. Crean, and B. Holben (2005a), MISR global aerosol optical depth validation based on two years of coincident AERONET observations, *J. Geophys. Res.*, *110*, D10S04, doi:10.1029/2004JD004706.

Kahn, R. A., et al. (2005b), MISR calibration, and implications for low-light level aerosol retrieval over dark water, *J. Atmos. Sci.*, *62*(4), 1032–1052, doi:10.1175/JAS3390.1.

Kahn, R. A., M. J. Garay, D. L. Nelson, K. K. Yau, M. A. Bull, B. J. Gaitley, J. V. Martonchik, and R. C. Levy (2007), Satellite-derived aerosol optical depth over dark water from MISR and MODIS: Comparisons with AERONET and implications for climatological studies, *J. Geophys. Res.*, *112*, D18205, doi:10.1029/2006JD008175.

Kahn, R. A., D. L. Nelson, M. J. Garay, R. C. Levy, M. A. Bull, D. J. Diner, J. V. Martonchik, S. R. Paradise, E. G. Hansen, and L. A. Remer (2009), MISR aerosol product attributes and statistical comparisons with MODIS, *IEEE Trans. Geosci. Remote Sens.*, *47*, 4095–4114, doi:10.1109/TGRS.2009.2023115.

Kalashnikova, O. V., and R. Kahn (2006), Ability of multiangle remote sensing observations to identify and distinguish mineral dust types: 2. Sensitivity over dark water, *J. Geophys. Res.*, *111*, D11207, doi:10.1029/2005JD006756.

Kaufman, Y. J., D. Tanré, L. A. Remer, E. Vermote, A. Chu, and B. N. Holben (1997), Operational remote sensing of tropospheric aerosol over land from EOS Moderate Resolution Imaging Spectroradiometer, *J. Geophys. Res.*, *102*(D14), 17,051–17,067, doi:10.1029/96JD03988.

Kinne, S. (2009), Remote sensing data combinations: Superior global maps for aerosol optical depth, in *Satellite Aerosol Remote Sensing over Land*, edited by A. A. Kokhanovsky and G. de Leeuw, pp. 361–381, Springer, Berlin, doi:10.1007/978-3-540-69397-0_12.

Kinne, S., et al. (2006), An AeroCom initial assessment—Optical properties in aerosol component modules of global models, *Atmos. Chem. Phys.*, *6*, 1815–1834, doi:10.5194/acp-6-1815-2006.

Levy, R. C., L. A. Remer, D. Tanré, Y. J. Kaufman, C. Ichoku, B. N. Holben, J. M. Livingston, P. B. Russell, and H. Maring (2003), Evaluation of the Moderate-Resolution Imaging Spectroradiometer (MODIS) retrievals of dust aerosol over the ocean using PRIDE, *J. Geophys. Res.*, *108*(D19), 8594, doi:10.1029/2002JD002460.

Levy, R. C., L. A. Remer, J. V. Martins, Y. J. Kaufman, A. Plana-Fattori, J. Redemann, and B. Wenney (2005), Evaluation of the MODIS aerosol retrievals over ocean and land during CLAMS, *J. Atmos. Sci.*, *62*(4), 974–992, doi:10.1175/JAS3391.1.

Levy, R. C., L. A. Remer, S. Mattoo, E. F. Vermote, and Y. J. Kaufman (2007), Second-generation operational algorithm: Retrieval of aerosol properties over land from inversion of moderate resolution imaging spectroradiometer spectral reflectance, *J. Geophys. Res.*, *112*, D13211, doi:10.1029/2006JD007811.

Liu, L., and M. I. Mishchenko (2008), Toward unified satellite climatology of aerosol properties: Direct comparisons of advanced level 2 aerosol products, *J. Quant. Spectrosc. Radiat. Transfer*, *109*(14), 2376–2385, doi:10.1016/j.jqsrt.2008.05.003.

Liu, Y., J. A. Sarnat, B. A. Coull, P. Koutrakis, and D. J. Jacob (2004a), Validation of Multiangle Imaging Spectro-radiometer (MISR) aerosol optical thickness measurements using Aerosol Robotic Network (AERONET) observations over the contiguous United States, *J. Geophys. Res.*, *109*, D06205, doi:10.1029/2003JD003981.

Liu, Y., R. J. Park, D. J. Jacob, Q. Li, V. Kilaru, and J. A. Sarnat (2004b), Mapping annual mean ground-level $PM_{2.5}$ concentrations using Multiangle Imaging Spectroradiometer aerosol optical thickness over the contiguous United States, *J. Geophys. Res.*, *109*, D22206, doi:10.1029/2004JD005025.

Liu, Y., M. Franklin, R. Kahn, and P. Koutrakis (2007), Using aerosol optical thickness to predict ground-level $PM_{2.5}$ concentrations in the St. Louis area: A comparison between MISR and MODIS, *Remote Sens. Environ.*, *107*(1-2), 33–44, doi:10.1016/j.rse.2006.05.022.

Loeb, N. G., W. Sun, W. F. Miller, K. Loukachine, and R. Davies (2006), Fusion of CERES, MISR, and MODIS measurements for top-of-atmosphere radiative flux validation, *J. Geophys. Res.*, *111*, D18209, doi:10.1029/2006JD007146.

Martonchik, J. V., D. J. Diner, R. Kahn, B. Gaitley, and B. N. Holben (2004), Comparison of MISR and AERONET aerosol optical depths over desert sites, *Geophys. Res. Lett.*, *31*, L16102, doi:10.1029/2004GL019807.

Martonchik, J. V., R. A. Kahn, and D. J. Diner (2009), Retrieval of aerosol properties over land using MISR observations, in *Satellite Aerosol Remote Sensing Over Land*, edited by A. A. Kokhanovsky and G. de Leeuw, pp. 267–293, Springer, Berlin, doi:10.1007/978-3-540-69397-0_9.

Mishchenko, M., I. V. Geogdzhayev, L. Liu, A. A. Lacis, B. Cairns, and L. D. Travis (2009), Toward unified satellite climatology of aerosol properties: What do fully compatible MODIS and MISR aerosol pixels tell us?, *J. Quant. Spectrosc. Radiat. Transfer*, *110*(6-7), 402–408, doi:10.1016/j.jqsrt.2009.01.007.

Myhre, G., Y. Govaerts, J. M. Haywood, T. K. Bernsten, and A. Lattanzio (2005), Radiative effect of surface albedo change from biomass burning, *Geophys. Res. Lett.*, *32*, L20812, doi:10.1029/2005GL022897.

Nguyen, H. (2009), Spatial statistical data fusion for remote-sensing applications, thesis, Univ. of Calif. Los Angeles, Los Angeles. (Available at http://theses.stat.ucla.edu/104/Data_fusion_Hai_Nguyen.pdf)

Paradise, S., B. Wilson, and A. Braverman (2010), The Aerosol Measurement and Processing System (AMAPS), *Earth Sci. Inform.*, *3*, 159–165, doi:10.1007/s12145-009-0042-7.

Penner, J. E., et al. (2002), A comparison of model- and satellite-derived optical depth and reflectivity, *J. Atmos. Sci.*, *59*(3), 441–460, doi:10.1175/1520-0469(2002)059<0441:ACOMAS>2.0.CO;2.

Prasad, A. K., and R. P. Singh (2007), Comparison of MISR-MODIS aerosol optical depth over the Indo-Gangetic basin during the winter and summer seasons (2000–2005), *Remote Sens. Environ.*, *107*(1–2), 109–119, doi:10.1016/j.rse.2006.09.026.

Remer, L. A., et al. (2005), The MODIS aerosol algorithm, products, and validation, *J. Atmos. Sci.*, *62*(4), 947–973, doi:10.1175/JAS3385.1.

Remer, L. A., et al. (2008), Global aerosol climatology from the MODIS satellite sensors, *J. Geophys. Res.*, *113*, D14S07, doi:10.1029/2007JD009661.

Vermote, E. F., J. C. Roger, A. Sinyuk, N. Saleous, and O. Dubovik (2007), Fusion of MODIS-MISR aerosol inversion for estimation of aerosol absorption, *Remote Sens. Environ.*, *107*(1–2), 81–89, doi:10.1016/j.rse.2006.09.025.

Xiao, N., T. Shi, C. A. Calder, D. K. Munroe, C. Berrett, S. R. Wolfinbarger, and D. Li (2009), Spatial characteristics of the difference between MISR and MODIS aerosol optical depth retrievals over mainland Southeast Asia, *Remote Sens. Environ.113*(1), 1–9 doi:10.1016/j.rse.2008.07.011.

Yu, H., et al. (2006), A review of measurement-based assessments of the aerosol direct radiative effect and forcing, *Atmos. Chem. Phys.*, *6*(3), 613–666, doi:10.5194/acp-6-613-2006.

Zapletal, M. (2001), Atmospheric deposition of nitrogen and sulphur compounds in the Czech Republic, *Sci. World J.*, *1*(2), 294–303.

A. J. Braverman, C. E. Miller, and S. R. Paradise, Jet Propulsion Laboratory, Pasadena, CA 91109, USA.

A. Chatterjee and A. M. Michalak, Department of Civil and Environmental Engineering, University of Michigan, Ann Arbor, MI 48109-2125, USA. (amichala@umich.edu)

R. A. Kahn, NASA Goddard Space Flight Center, Greenbelt, MD 20771, USA.